Transverse pattern formation of optical vortices in a microchip laser with a large Fresnel number

Y. F. Chen*
Department of Electrophysics, National Chiao Tung University, Hsinchu, Taiwan, Republic of China

Y. P. Lan
Institute of Electro-Optical Engineering, National Chiao Tung University, Hsinchu, Taiwan, Republic of China
(Received 11 June 2001; published 5 December 2001)

We experimentally investigate the dependence of the transverse pattern formation in a solid-state microchip laser on the Fresnel number. Controlling the transverse-mode spacing and the mode size can generate the stable transverse pattern of optical vortex lattices. A spontaneous process of transverse-mode locking within almost-degenerated mode families is found in the formation of vortex lattices. The frequency of self-induced oscillation in vortex lattices agrees well with the previous theoretical prediction.

DOI: 10.1103/PhysRevA.65.013802 PACS number(s): 42.55.Px, 42.65.Sf, 42.60.Mi

I. INTRODUCTION

Pattern formation and nonlinear dynamics have been widely investigated in many different fields, including hydrodynamics, chemical reactions, and optics [1,2]. Recent experiments have identified two types of pattern formation on photorefractive oscillators, one that is controlled by the boundary conditions (cavity mirrors), and another by the nonlinearity of the medium [3,4]. If the optical system is boundary controlled, the transverse patterns can be successfully described in terms of the empty cavity eigenmodes. On the other hand, the pattern formation in nonlinearity-controlled regimes is in general described by the complex Swift-Hohenberg equation (CSHE) that is a universal order-parameter equation for the nonlinear optical systems with large Fresnel numbers, such as class-A lasers, optical parametric oscillators, and photorefractive oscillators [5,6]. Typical patterns of the CSHE include vortices, domains of tilted waves, and square patterns [6]. However, it is difficult experimentally to observe the nonlinearity-controlled patterns in laser systems because the requirements comprise both a large Fresnel number of the resonator and a high level of degeneracy of transverse-mode families.

Pattern formation in class-B lasers, such as CO_2 and solid-state lasers, has attracted much interest since the inertial nonlinearity may induce other instabilities. In class-B lasers, the population inversion acts as a mean flow, driving the active modes at finite wave number. It has been found that the behavior of class-B lasers can be described by coupling the population inversion dynamics with the CSHE [7,8]. Although complicated transverse structures appeared in CO_2 lasers, the patterns observed so far could be interpreted as the simultaneous excitation of empty cavity eigenmodes [9,10]. This implies that the patterns were dominated by boundary effects, rather than by the nonlinearity of the medium. In addition, experimental works in CO_2 lasers usually used long cavities in which the longitudinal-mode spacing is of the same order of magnitude as the transverse-mode spacing [11]. The presence of several longitudinal modes probably constituted the main reason for the discrepancies between theoretical predictions and experimental observations. Recently, vertical cavity surface emitting semiconductor lasers (VCSEL's) of large transverse section and short cavity length have been used to study the pattern formation [12]. The VCSEL's emit a single-longitudinal-mode wave because of their short cavities. The single-longitudinal-mode laser is a useful laboratory to study transverse phenomena without the influence of other degrees of freedom. However, the main difficulty for analysis is that the pattern formation is strongly sensitive to the homogeneity of the processed wafer.

The recent rapid progress of diode-pumped microchip lasers has driven a renaissance of solid-state laser-physics research and led to novel phenomena [13,14]. The diode-pumped microchip laser can be easily operated in single-longitudinal mode more than ten times above threshold before the second longitudinal mode reaches threshold because the microchip gain medium has a short absorption depth that reduces the longitudinal spatial-hole burning effect [15,16]. In previous works [14], we used a doughnut-shaped pump profile to generate the high-order Laguerre-Gaussian (LG) transverse-electromagnetic mode ($TEM_{0,l}$) and $TEM^*_{0,l}$ modes in an end-pumped microchip laser, where l is the azimuthal index of the LG mode. A rich set of dynamical behaviors, such as periodic and quasiperiodic self-modulation, chaotic pulsing, and frequency locking, has been experimentally observed in the generated $TEM^*_{0,l}$ hybrid mode. The bifurcation mechanisms have been theoretically investigated from the Maxwell-Bloch equations. It was found that the relaxation oscillation plays an important role not only in transient processes, but also in the appearance of dynamic chaos.

In this work, the transverse structure of the output beam of the microchip laser evolves with the Fresnel number Fr and the transverse-mode spacing $\Delta\nu_T$. A fiber-coupled laser diode with top-hat emission profile is used to excite a high level of degeneracy of transverse modes. At low Fresnel number, typically $Fr \leqslant 10$, the transverse pattern near the lasing threshold could exhibit concentric-ring pattern that could

*Author to whom correspondence should be addressed: Department of Electrophysics, National Chiao Tung University, 1001 TA Hsueh Road, Hsinchu, Taiwan, 30050. FAX: (886-35) 729134. Email address: yfchen@cc.nctu.edu.tw

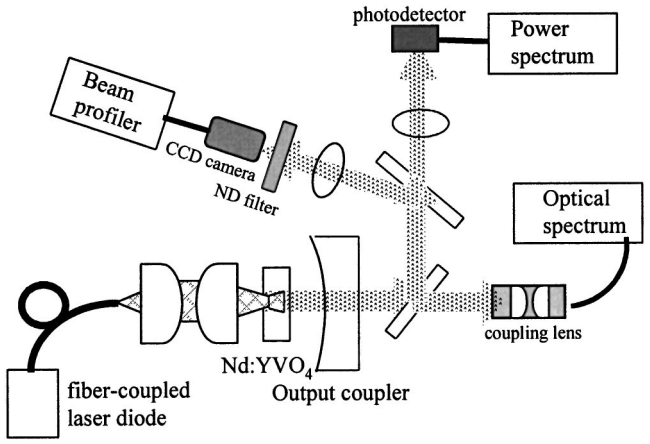

FIG. 1. Schematic of a fiber-coupled diode end-pumped laser, a typical beam profile of a fiber-coupled laser diode away from the focal plane.

be described as a function of modes of the empty cavity with the rules of transverse-hole burning [10]. On the other hand, for Fr$>$15, the characteristic pattern is the so-called ''square pattern'' (square vortex lattice) that has been theoretically predicted in lasers with large Fresnel numbers. Experimental results reveal that the stability of transverse patterns significantly depends on the transverse-mode spacing $\Delta\nu_T$. The transverse-mode locking is found when the average nearest-neighbor separation between vortices is less than $\sim$0.07 mm.

II. EXPERIMENT

Figure 1 shows the schematic of an end-pumped microchip laser considered in this work. The gain medium is a cut 2.0-at. % 1-mm-long Nd:YVO_4 crystal. The absorption coefficient of the Nd:YVO_4 crystal is about 60 cm^{-1} at 809 nm. We used a plano-concave cavity that consists of one planar Nd:YVO_4 surface, high-reflection coated at 1064 nm and high-transmission coated at 809 nm for the pump light to enter the laser crystal, and a spherical output mirror. The second surface of the Nd:YVO_4 crystal is antireflection coated at 1064 nm. The output coupler is a concave mirror with the reflectivity of 98.5%. We setup the resonator length to be as short as possible for reaching single-longitudinal-mode operation. The total length in the present resonator is $\sim$2.5 mm. The frequency spacing between consecutive longitudinal modes $\Delta\nu_L$ is about 60 GHz. Since the longitudinal-mode spacing is considerably greater than the transverse-mode spacing, the present laser can be easily operated in single-longitudinal mode to study the pattern formation.

The pump source is a 1 W fiber-coupled laser diode (Coherent, F-81-800C-100) with a 0.1 mm of core diameter. Note that the intensity profile of the fiber-coupled laser diode, depending on the coupling condition, can be a top-hat distribution or a doughnut distribution. In previous work, we used a doughnut pump profile to generate high-order LG $TEM_{0,l}$ and $TEM^{*}_{0,l}$ modes. Here we use a top-hat emission profile to excite a high level of degeneracy of transverse modes. The pump power was focused into the Nd:YVO_4 crystal by using a focusing lens with 0.57 magnification.

The Fresnel number can be given by $\mathrm{Fr}=a^2/(\pi\omega_o^2)$, where $\pi\omega_o^2$ is the area of the lowest-order mode cross. For an end-pumped microchip laser, the effective aperture is usually determined by the pump cross section not by the mirror aperture. Namely, the Fresnel number for an end-pumped microchip laser is given by $\mathrm{Fr}=\omega_p^2/(\pi\omega_o^2)$, where ω_p is the pump size on the gain medium. Changing the pump-to-mode size ratio ω_p/ω_o can, therefore, control the value of Fresnel number. For the present cavity, the mode size on the microchip is given by

$$\omega_o^2=\frac{\lambda}{\pi}\sqrt{L(R-L)}, \tag{1}$$

where R is the radius of curvature of the output coupler. Three different output couplers are used in the experiment, the radii of curvature are 250 mm, 50 mm, and 10 mm, respectively. For $L=2.5$ mm, the mode size on the microchip is calculated to be 0.092 mm, 0.061 mm, and 0.038 mm, respectively, for $R=250$ mm, $R=50$ mm, and $R=10$ mm. Defocusing the pump source, the pump size can be adjusted within $0.1\sim0.75$ mm. The maximum pump size depends on the lasing threshold. Using $\lambda=1.064\,\mu$m and $L=2.5$ mm, the Fresnel number can vary from 0.5 to 25 for $R=250$ mm. On the other hand, the Fresnel number can vary from 2 to 125 for $R=10$ mm. Note that the thermal lensing effect is not significant because the thermal power density on the gain medium is controlled to be less than 0.5 W/mm^2.

In addition to the Fresnel number, the transverse-mode spacing $\Delta\nu_T$ plays another dominant role in the dynamics of transverse patterns. The transverse-mode spacing governs the coupling strength between the transverse modes, and thus rules the influence of the nonlinearity on the dynamical behavior. For the present cavity, the transverse-mode spacing is given by

$$\Delta\nu_T=\Delta\nu_L\left[\frac{1}{\pi}\cos^{-1}\left(\sqrt{1-\frac{L}{R}}\right)\right]. \tag{2}$$

For $\Delta\nu_L=60$ GHz and $L=2.5$ mm, the transverse-mode spacing is found to be 1.9 GHz, 4.3 GHz, and 10 GHz, respectively, for $R=250$ mm, $R=50$ mm, and $R=10$ mm.

III. RESULTS AND DISCUSSION

First we used an output coupler with $R=250$ mm in the laser cavity. At low Fr (Fr$<$10), the laser emits the successive concentric ring patterns near lasing threshold, as shown in Fig. 2. The vortices that appear between the bright rings are a signature of the presence of a great number of phase singularities. The similar concentric ring patterns have been observed in CO_2 lasers. Louvergneaux *et al.* [10] evidenced that the concentric ring pattern can be described as a function of the Hermite-Gausian $TEM_{m,n}$ modes of the empty cavity with the following rules: (i) all modes belong to the same family $q=m+n\approx\mathrm{Fr}$, (ii) in this family, transverse modes associate in the laser to maximize energy and simultaneously minimize overlapping between their intensity distribution,

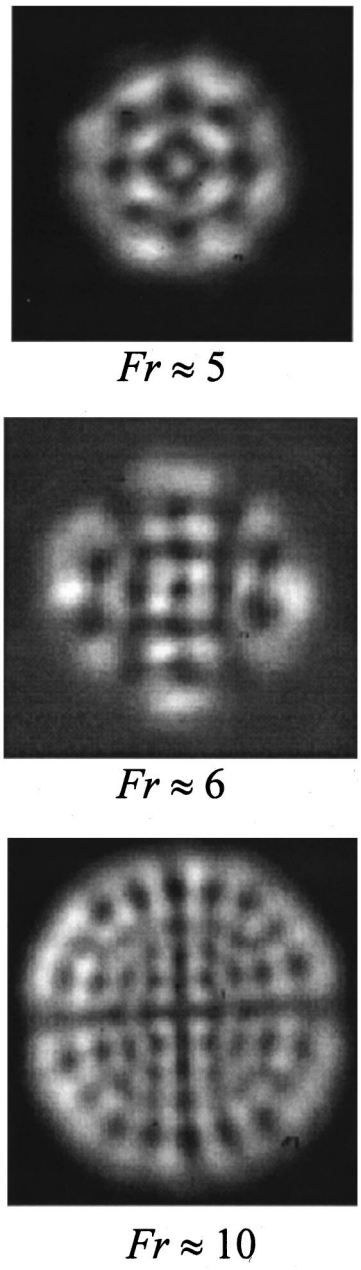

FIG. 2. Beam profiles of laser emission for three concentric ring patterns near lasing threshold, measured with the CCD camera.

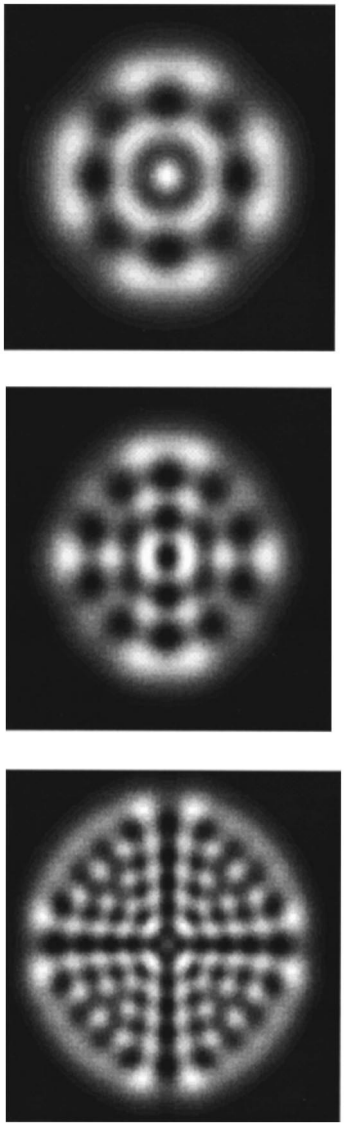

FIG. 3. The numerically reconstructed patterns for the results shown in Fig. 2, calculated with the selection rules given by Louvergneaux *et al.* [10].

(iii) all modes have equal weight. Basically, these selection mechanisms are shown to be transverse spatial-hole burning. With the rules given by Louvergneaux *et al.* [10], the patterns shown in Fig. 2 were numerically reconstructed, as depicted in Fig. 3. The good agreement between the experimental and reconstructed patterns indicates that the transverse patterns are boundary controlled.

The temporal behavior is recorded by a power-spectrum analyzer and a fast Si *p-i-n* photodiode with a rise time of less than 1 ns. There are several characteristic relaxation oscillations appearing in the measured power spectra for the concentric ring patterns near lasing threshold, as shown in Fig. 4(a). Increasing the pump power, the vortices in the concentric ring patterns tend to annihilate and nucleate, additional relaxation oscillations and beat frequencies appear in the power spectra, as shown in Figs. 4(b) and 4(c). Further increasing the pump power, the spectra broaden with a transition to chaotic relaxation oscillations, as shown in Fig. 4(d). The appearance of dynamic chaos is believed to arise from the interaction of the relaxation frequency and the frequency difference between the nearly degenerate modes. In the present cavity, the frequency difference between the nearly degenerate modes may be caused by the cross-saturation and other astigmatism. A nonlinear system of the Maxwell-Bloch equations [17] was used to investigate the interaction of two nearly degenerate transverse modes in a class-B laser. It is found that there is a chaotic set of solutions when the frequency difference is close to the relaxation frequency.

At large Fr ($Fr > 15$) the transverse structure is spontaneously modified to a square pattern, i.e., a square vortex lat-

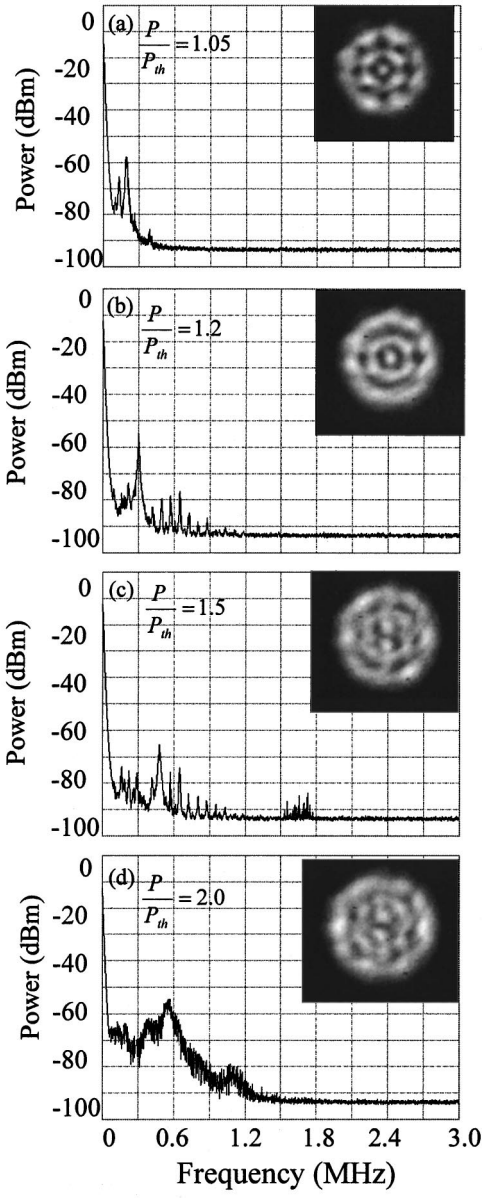

FIG. 4. Power-intensity spectra of laser emission at Fr≈5 and $\Delta\nu_T=1.9$ GHz; (a) near lasing threshold, (b) 1.2 times above threshold, (c) 1.5 times above threshold, (d) 2.0 times above threshold. Beam profiles of laser emission are shown in the insets.

tice, as shown in Fig. 5(a) for Fr≈25. The orientation of the optical axes of the gain medium determines the axes of the square pattern. As shown in Fig. 5(b), a chaotic regime could also occur and the vortices in the square pattern annihilate and nucleate when the pump power is slightly increased.

To investigate the influence of transverse-mode spacing $\Delta\nu_T$, we replaced the output coupler with a $R=50$ mm concave mirror. The $\Delta\nu_T$ changes from 1.9 GHz to 4.3 GHz at the same cavity length. Near the lasing threshold, the dependence of pattern formations on the Fresnel number is almost identical as the previous result except that a larger square pattern can be emitted due to a smaller mode size. Even so, the dynamics of the transverse patterns are completely different not only at lasing threshold but far above threshold.

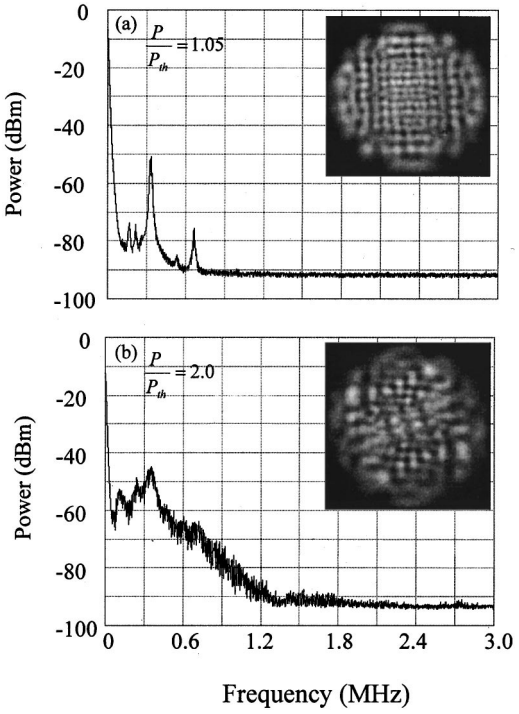

FIG. 5. Power-intensity spectra of laser emission for the square pattern at Fr≈25 and $\Delta\nu_T=1.9$ GHz, (a) near lasing threshold, (b) two times above threshold. Beam profiles are shown in the insets.

Figures 6(a) and 6(b) depict, respectively, the results of the power spectra just near and two times above lasing threshold for the square pattern with Fr≈50. It can be found that the

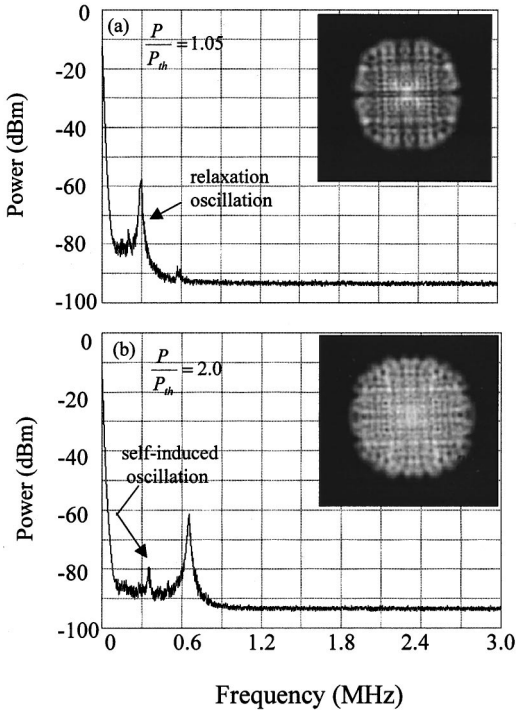

FIG. 6. Power-intensity spectra of laser emission for the square pattern at Fr≈50 and $\Delta\nu_T=4.3$ GHz, (a) near lasing threshold, (b) two times above threshold. Beam profiles are shown in the insets.

temporal behavior is similar to the dynamics of single-transverse mode in class-B lasers except that there is an additional oscillation component with frequency lower than the relaxation frequency. The power spectrum is also found to be almost independent of the region of the laser-pattern detected. This result indicates that the present square pattern can be described as emanating from a spontaneous process of transverse-mode locking of nearly degenerate modes. In addition to $\Delta\nu_T$, the other control parameter for transverse-mode locking is the average nearest-neighbor separation D_{av} between phase singularities (or bright spots), which is proportional to $\omega_o/\sqrt{\mathrm{Fr}}$ and represents the characteristic length of the transverse pattern. The experimental result shows that D_{av} should be less than $\sim$0.07 mm for transverse-mode locking. This value is close to the characteristic length of the inverse gain coefficient $1/(\sigma N)$, where σ is the stimulated emission cross section of the gain medium and N is the active-ion concentration of the gain medium. For the a cut 2.0-at. % Nd:YVO_4 crystal, $\sigma=16.5\times10^{-19}\,\mathrm{cm}^2$, and $N=2.5\times10^{20}\,\mathrm{cm}^{-3}$. Note that the inverse of the gain coefficient represents the mean distance between the stimulated emissions. The criterion for transverse-mode locking is more rigorous than the result found in the phase locking of two-coupled lasers [18–20] in which the separation for mutual coherent needs to be less than 0.35 mm in the regime of megahertz detunings. Although similar transverse locking in the generation of optical vortex crystals was demonstrated in broad-area VCSELs [21], optical systems so far have not generated such a large number of vortices in a single-mode emission. An additional oscillation mode in the power spectrum of Fig. 6 may be interpreted as the ''acoustic'' oscillation mode that resembles the oscillation of atoms in alkali-halide-type crystal when an acoustic phonon is excited. The theoretical analysis [8] show that there are two pure-vibrational modes of the self-induced dynamics of vortex lattices: (1) ''acoustic'' oscillation mode, where the neighboring vortices along a diagonal oscillation in phase; (2) ''optical'' oscillation mode, where the neighboring vortices along a diagonal oscillation in antiphase. The acoustic mode is the oscillation that only the transverse modes from the same degenerate family are involved, whereas the optical oscillation mode occurs when the transverse modes from two different families are simultaneously excited. Since the present transverse pattern emanates from a high level of degeneracy of transverse-mode families, the self-induced oscillation should belong to the acoustic mode. The numerical calculation [8] shows that the frequency of the acoustic oscillation is smaller by a factor of about $2\sqrt{2}$ than the relaxation oscillation frequency. As shown in Fig. 6, the experimental result agrees very well with the theoretical prediction.

Increasing $\Delta\nu_T$ to 10 GHz by use of a $R=10$-mm output coupler, the pattern formations and dynamics are roughly similar to the results of $\Delta\nu_T=4.3$ GHz, as depicted in Fig. 7 Fr$\approx$125. Nevertheless, we stress that the power spectra are almost free of noise peaks in comparison with the result shown in Fig. 6. This result further confirms that the transverse-mode spacing plays a primary role on the stability of the transverse pattern within quasidegenerated mode families.

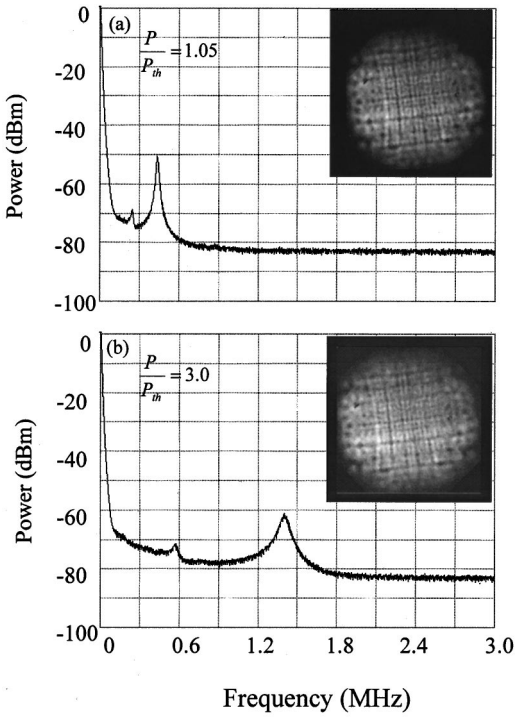

FIG. 7. Power-intensity spectra of laser emission for the square pattern at Fr$\approx$125 and $\Delta\nu_T=10$ GHz, (a) near lasing threshold, (b) three times above threshold. Beam profiles are shown in the insets.

Finally, it is worthwhile to mention that an additional frequency is also found in the power spectra of Fig. 7. The theoretical analysis for the vortex trajectory show that the self-induced oscillation mode can be found in a class-B laser if and only if the spectrum width of the lasing frequency needs to be less than the relaxation oscillation frequency. This criterion is consistent with the experimental result that the transverse-mode locking is an indispensable process of finding the unique additional frequency accompanied by the relaxation oscillation frequency in the square pattern. Furthermore, it is experimentally found that the additional frequency generally has the same pump-power dependence as the relaxation oscillation. The power spectrum is also found to be almost independent of the region of the laser-pattern detected. The consistence in the optical spectra and the regularity in the power spectra constitute a plausible support that the additional frequency is interpreted as a self-induced oscillation mode of the vortex lattices.

IV. CONCLUSIONS

We investigated the dynamics of transverse patterns in solid-state microchip lasers with a large Fresnel number. The dependence of pattern formations on the Fresnel number is demonstrated. When $\Delta\nu_T<2$ GHz, the spatial symmetries of transverse patterns are destroyed at higher pump power. When $\Delta\nu_T>4$ GHz and $D_{\mathrm{av}}<0.07$ mm, the vortices in the transverse patterns do not annihilate and nucleate and the dynamics of the transverse patterns are not the results of multimode operation but exhibit single-transverse-mode characteristics. The transverse pattern could be described as

a spontaneous process of transverse-mode locking of nearly degenerate modes, assisted by the nonlinearity of gain medium. Moreover, the dynamics of the square pattern agrees very well with the theoretical prediction.

ACKNOWLEDGMENT

The authors thank the National Science Council of the Republic of China for financially supporting this research under Contract No. NSC-90-2112-M-009-034.

[1] Chaos, Solitons Fractals **4**, 1249 (1994) special issue on Nonlinear Optical Structure, Patterns, Chaos edited by L. A. Lugiato.
[2] M. C. Cross and P. C. Hohenberg, Rev. Mod. Phys. **65**, 851 (1993).
[3] F. T. Arecchi, S. Boccaletti, P. L. Ramazza, and S. Residori, Phys. Rev. Lett. **15**, 2277 (1993).
[4] K. Staliunas, G. Slekys, and C. O. Weiss, Phys. Rev. Lett. **79**, 2658 (1997).
[5] A. C. Newell, in *Spatio-Temporal Patterns in Nonequilibrium Complex Systems*, edited by P. E. Gladis and P. Palffy-Muhoray (Addison-Wesley, Reading, MA, 1993), Vol. XXI.
[6] K. Staliunas and C. O. Weiss, Physica D **81D**, 79 (1995).
[7] J. Lega, J. V. Moloney, and A. C. Newell, Phys. Rev. Lett. **73**, 2978 (1994).
[8] K. Staliunas and C. O. Weiss, J. Opt. Soc. Am. B **12**, 1142 (1995).
[9] D. Dangoisse, D. Hennequin, C. Lepers, E. Louvergneaux, and P. Glorieux, Phys. Rev. A **46**, 5955 (1992).
[10] E. Louvergneaux, D. Hennequin, D. Dangoisse, C. Lepers, and P. Glorieux, Phys. Rev. A **53**, 4435 (1996).
[11] G. Huyet, C. M. Martinoni, J. R. Tredicce, and S. Rica, Phys. Rev. Lett. **75**, 4027 (1995).
[12] S. P. Hegarty, G. Huyet, P. Porta, J. G. McInerney, K. D. Choquette, K. M. Geib, and H. Q. Hou, J. Opt. Soc. Am. B **16**, 2060 (1999).
[13] K. Otsuka, P. Mandel, and E. A. Viktorov, Phys. Rev. A **56**, 3226 (1997).
[14] Y. F. Chen and Y. P. Lan, Phys. Rev. A **63**, 063807 (2001).
[15] J. J. Zayhowski, IEEE J. Quantum Electron. **26**, 2052 (1990).
[16] G. J. Kintz and T. Baer, IEEE J. Quantum Electron. **26**, 1457 (1990).
[17] D. V. Skryabin, A. G. Vladimirov, and A. M. Radin, Quantum Electron. **27**, 892 (1997).
[18] L. Fabiny, P. Colet, and R. Roy, Phys. Rev. A **47**, 4287 (1993).
[19] K. S. Thornburg, Jr., M. Moller, R. Roy, T. W. Carr, R. D. Li, and T. Erneux, Phys. Rev. E **55**, 3865 (1997).
[20] M. Moller, B. Forsmann, and W. Lange, Quantum Semiclassic. Opt. **10**, 839 (1998).
[21] J. Scheuer and M. Orenstein, Science **285**, 230 (1999).